energies

MDPI

Article

A Method to Monitor IGBT Module Bond Wire Failure Using On-State Voltage Separation Strategy

Qingyi Kong [1], Mingxing Du [1,*], Ziwei Ouyang [1,2], Kexin Wei [1] and William Gerard Hurley [1,3]

1 Tianjin Key Laboratory of Control Theory & Applications in Complicated System, Tianjin University of Technology, Tianjin 300384, China; Kqy731bj@163.com (Q.K.); zo@elektro.dtu.dk (Z.O.); kxwei@tjut.edu.cn (K.W.); gerard.hurley@nuigalway.ie (W.G.H.)
2 Department of Electrical Engineering, Technical University of Denmark, 2800 Kgs Lyngby, Denmark
3 Department of Electrical Engineering, The National University of Ireland, H91 TK33 Galway, Ireland
* Correspondence: dumx@tjut.edu.cn; Tel.: +86-22-60214268

Received: 7 April 2019; Accepted: 7 May 2019; Published: 11 May 2019

Abstract: On-state voltage is an important thermal parameter for insulated gate bipolar transistor (IGBT) modules. It is employed widely to predict failure in IGBT module bond wires. However, due to restrictions in work environments and measurement methods, it is difficult to ensure the measurement accuracy for the on-state voltage under practical working conditions. To address this problem, an on-state voltage separation strategy is proposed for the IGBT modules with respect to the influence of collector current (I_c) and junction temperature (T_j). This method involves the separation of the on-state voltage into a dependent part and two independent parts during the IGBT module bond wire prediction. Based on the proposed separation strategy, the independent parts in the failure prediction can be removed, making it possible to directly monitor the voltage variations caused by bond wire failure. The experimental results demonstrate that the proposed diagnosis strategy can accurately predict the bond wire failure stage in an IGBT module under different conditions.

Keywords: insulated gate bipolar transistor (IGBT) module; bond wire failure; on-state voltage; separation strategy

1. Introduction

In recent years, power electronic systems have been widely used in various fields that require high stability, e.g., wind power [1,2], electric vehicles [3,4], ship manufacturing [5], and aerospace engineering [6]. The literature has shown that optional semiconductor device failures account for 31% of all faults in power electronic systems [7]. An insulated gate bipolar transistor (IGBT) module, which is a widely used semiconductor device in power converters [8], plays an important role in the reliability of power electronic system. In some fields, IGBT modules have to endure more than five million power cycles during their lifetimes [9], which makes failure inevitable. The failure rate of IGBT modules also increases in harsh operating environments and with higher voltage levels [10,11]. Therefore, it is important to study the aging mechanism of IGBT modules and propose an accurate method to monitor the aging process to improve the reliability of the whole power electronic converter.

Since IGBT modules switch continuously for a specific period during operation, the junction temperature fluctuates in a range far higher than that of the operating temperature [12]. Due to the different thermal expansion coefficients of different materials [13], tremendous thermal stress is generated by the temperature swing, which causes aging of the IGBT module [14,15]. The principal phenomenon involved in the aging process of IGBT modules is bond wire failure. It is also an important factor affecting the reliability of the modules. This failure consists of bond wire liftoff and cracking [16]. When one bond wire fails, the other bond wires suffer more intensive current density, which accelerates

the aging process of the IGBT module as a whole and eventually triggers the breakdown of the power electronic converter. Therefore, using appropriate methods to predict the aging failure of IGBT modules [17–20] can improve the reliability of power electronic systems.

Studies have shown that bond wire failure leads to an increase in the resistance of the bond wire, consequently leading to an increase in the on-state voltage [21]. Thus, measuring the on-state voltage while the IGBT is in operation [22,23] can be used to predict bond wire failure. Generally, additional external circuits [24,25] are widely used in voltage regulation element (V_{ce}) monitoring to predict IGBT bond wire failure. However, all these methods increase the complexity of the power electronic system. References [26,27] concentrate on the intersecting voltage ($V_{ce\text{-}int}$) of the I–V characteristic curves at different operating temperatures to predict IGBT module bond wire failure. However, it is a big challenge to apply $V_{ce\text{-}int}$ to predict IGBT module bond wire failure in other working conditions. By considering the influence of temperature on V_{ce}, a function can be used to describe the relationship between V_{ce} and temperature [28], thereby providing a method to predict IGBT module bond wire failure.

Based on previous research and an investigation of the internal structure and conduction mechanism of IGBT modules, this paper proposes an on-state collector-emitter voltage separation method. This method considers the influence of collector current and changes in junction temperature on each part of the voltage and is capable of calculating the on-state voltage of each part under different working conditions. The experimental results demonstrate that this separation strategy is accurate enough for IGBT module bond wire failure prediction.

The paper is organized as follows. Section 2 analyzes the on-state voltage separation strategy, based on the physical structure and the influence of the junction temperature on different components of the on-state voltage. The extraction method for the parameters required in the proposed on-state voltage separation strategy is covered in Section 3. In Section 4, the proposed separation strategy is employed to predict IGBT module bond wire failure. The experimental results demonstrate the accuracy of this method for bond wire prediction. Section 5 provides a summary and conclusions.

2. The On-State Voltage Separation Strategy

2.1. On-State Voltage Model for IGBT Module

Starting from the physical structure of the IGBT module, the on-state voltage is divided into chip level voltage and package level voltage. The package level voltage is strongly influenced by IGBT module bond wire failure—neither bond wire crack nor liftoff decreases access to current, implying an increase in package resistance, as well as in the package level voltage and the on-state voltage.

In [29], the on-state voltage was separated in a more detailed model. It provides a method to calculate the on-state voltage under different collector current (I_c) conditions:

$$V_{ce} = V_{ce\text{-}th} + V_{on\text{-}chip} + V_{package} \tag{1}$$

$$V_{on\text{-}chip} = R_{on\text{-}chip} \times I_c \tag{2}$$

$$V_{package} = R_{package} \times I_c \tag{3}$$

where the $V_{ce\text{-}th}$ is the collector-emitter threshold voltage, $V_{on\text{-}chip}$ is the on-state chip voltage, $V_{package}$ is the package voltage, $R_{on\text{-}chip}$ is the on-state chip resistance, and $R_{package}$ is the package resistance. However, I_c is not the only factor that influences on-state voltage. The voltage is also affected by the junction temperature, which fluctuates under real working conditions. We further consider the influence of both the collector current and junction temperature on on-state voltage in the following sections.

2.2. Influence of Temperature on On-State Voltage

On-state voltage is a temperature sensitive parameter in IGBT modules. The relationship between the on-state voltage and junction temperature is shown in Figure 1. There is an intersection point

($V_{ce\text{-}int}$) in the voltage curves that indicates the influence of the collector current (I_c) and junction temperature (T_j). When V_{ce} is less than $V_{ce\text{-}int}$, V_{ce} decreases as T_j increases and has a negative temperature coefficient. When V_{ce} is greater than $V_{ce\text{-}int}$, V_{ce} behaves in a completely different manner and has a positive temperature coefficient.

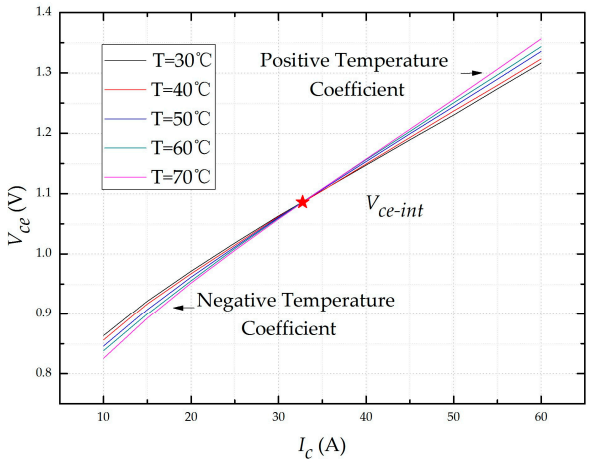

(**a**)

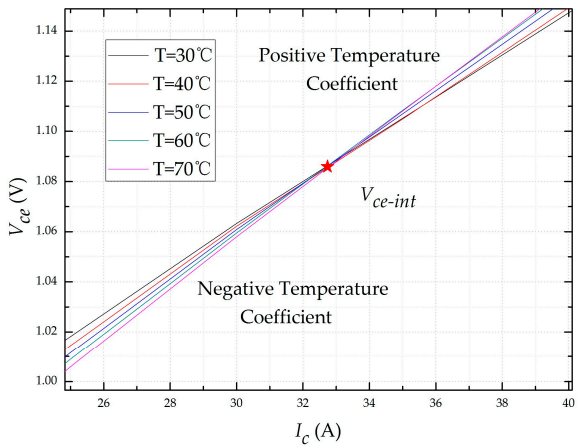

(**b**)

Figure 1. Relationship between on-state voltage (Vce) and junction temperature (T_j): (**a**) The complete characteristic curves; (**b**) the enlarged view near an intersection point ($V_{ce\text{-}int}$).

$V_{ce\text{-}th}$ is the emitter-collector threshold voltage of the IGBT module. It remains constant as I_c increases, but decreases as T_j increases. The V–I characteristic curves for different junction temperatures are shown in Figure 2. A method introduced in reference [29] extracts $V_{ce\text{-}th}$ using the V–I characteristic curves. We adopted this method to acquire threshold voltages under different junction temperatures, as shown in Figure 3.

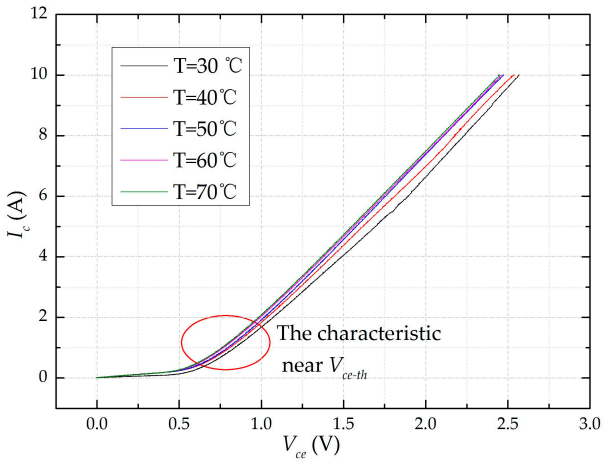

(**a**)

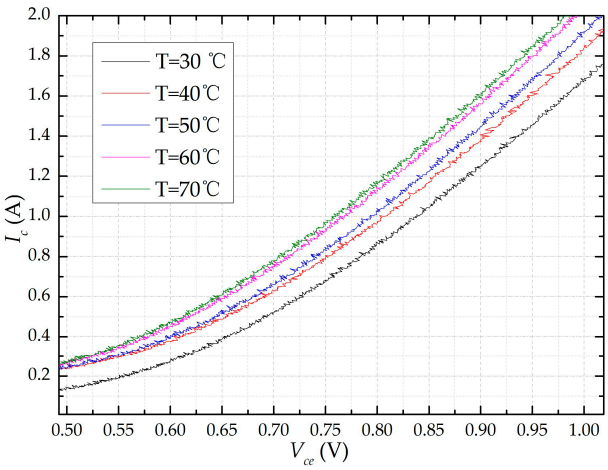

(**b**)

Figure 2. V–I characteristic curves at different junction temperatures: (**a**) The whole part of the characteristic curves; (**b**) the enlarged view near $V_{ce\text{-}th}$.

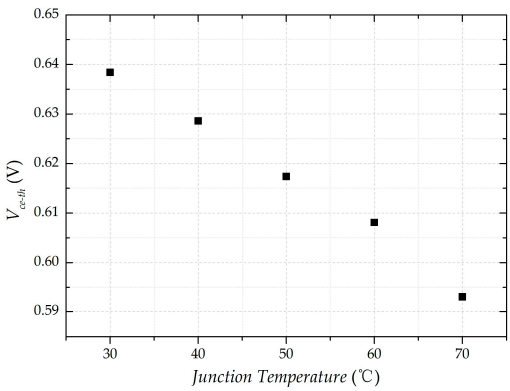

Figure 3. Threshold voltages at different junction temperatures.

When the temperature is taken to be an independent variable, the dependent variable is the electrical resistivity of the metal. The thermal motion of the lattice inside the metal becomes more intensive with an increasing temperature, making it more chaotic. The obstruction of free electrons

increases resistivity; thus, $R_{package}$ has a positive temperature coefficient, and the resistance of Al bond wires (T_0 = 228) at different junction temperatures can be obtained by Equation (4):

$$r_{k75°C} = r_{k\theta}\frac{T_0 + 75}{T_0 + \theta} \tag{4}$$

where $r_{k75°C}$ is the resistance at 75 °C and $r_{k\theta}$ is the resistance in standard temperature. In [29], $R_{package}$ was extracted at the room temperature; thus, θ in Equation (4) was 25 °C and $r_{k\theta}$ = 2.146 mΩ. Then, we obtained the $V_{package}$ at different junction temperatures, as shown in Figure 4.

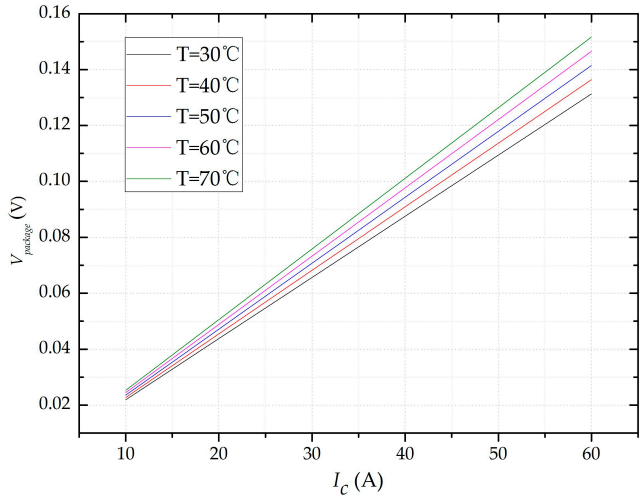

Figure 4. Package voltages at the different junction temperatures.

$V_{on\text{-}chip}$ is the on-state chip voltage which can be obtained from Equation (1). The collector current influence and the junction temperature were both considered, as shown in Figure 5.

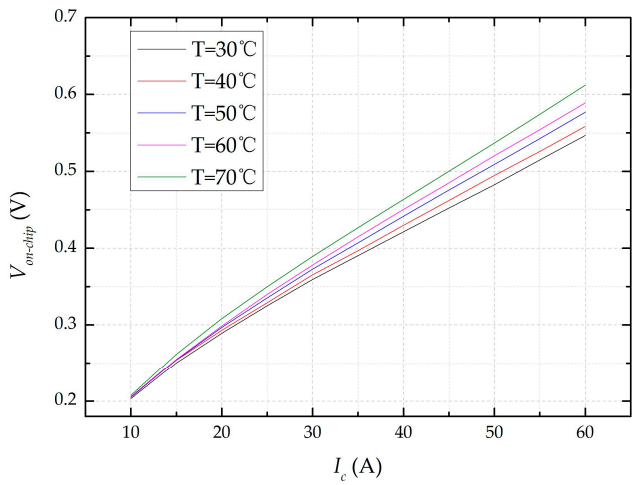

Figure 5. On-state chip voltages at different junction temperatures.

An updated model was generated for the on-state voltage, showing the influences of I_c and T_j in order to obtain V_{ce} under different conditions:

$$V_{ce}\ (I_c,T_j) = V_{ce\text{-}th}\ (T_j) + V_{on\text{-}chip}\ (I_c,T_j) + V_{package}\ (I_c,T_j). \tag{5}$$

3. Measurements of On-State Voltage

3.1. Experimental Setup

Figure 6 shows the on-state voltage acquisition system. A high-power DC power source was connected in series with electronic loads on both sides of the collector-emitter. Another DC power source was connected to the gate-emitter of the IGBT module. A high-low temperature test chamber was used to achieve the temperature control for the IGBT module. The on-state voltage was measured using digital multimeters.

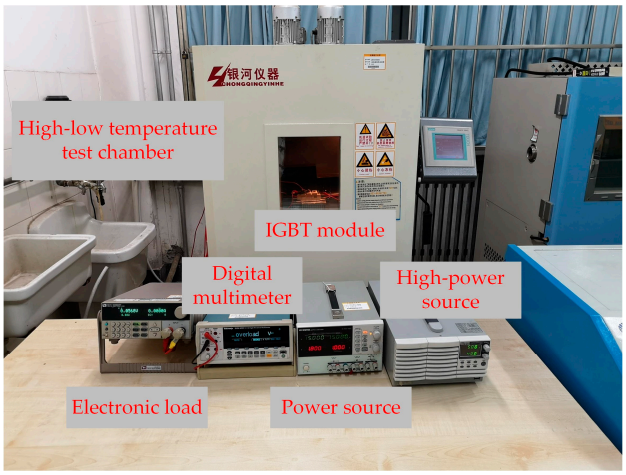

Figure 6. The on-state voltage acquisition system.

Figure 7 shows the semiconductor parameter test system, which is composed of a 2651A high power system sourcemeter, a 2636B system sourcemeter, an 8010 high power test device, and a microcomputer. The 8010 high power test device was used to connect 2600B and 2651A with the IGBT module and computer. Finally, V–I characteristic curves for the IGBT module were obtained by ACS software (V2.0 Release, Keithley Instruments, Cleveland, Ohio, USA).

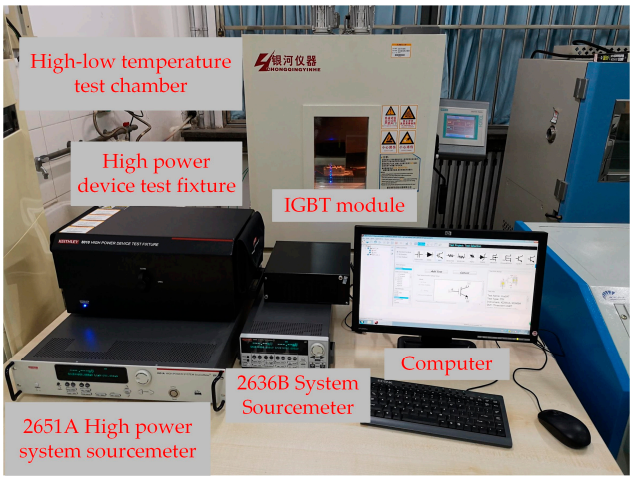

Figure 7. The semiconductor parameter test system.

A custom-made IGBT module (with the package removed) from Guoyang Electronics (WGL100B65F23) was used, as shown in Figure 8.

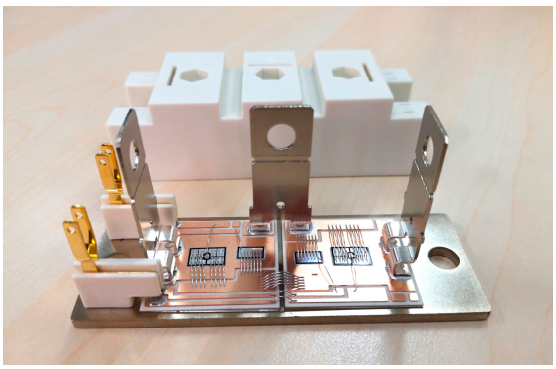

Figure 8. The insulated gate bipolar transistor (IGBT) module used in the experiment.

3.2. Acquisition of the Collector-Emitter Threshold Voltage

The experimental temperatures for the high-low temperature test chamber were set as 30 °C to 70 °C. The results are shown as V–I characteristic curves in Figure 2. The relationship between V_{ce} and I_c became linear after a period of time when the IGBT module reached the on-state status. We adopted the method in Reference [29] to extract $V_{ce\text{-}th}$ at different junction temperatures. The results are as shown in Figure 3. Their relationships were fitted with the function; the detailed data are listed in Table 1. $V_{ce\text{-}th}$ has a negative temperature coefficient that can be approximated by a liner relationship. Thus, it was possible to obtain $V_{ce\text{-}th}$ at different junction temperatures with low errors after acquiring the function in Equation (6).

$$V_{ce\text{-}th}\left(T_j\right) = -0.00112 \times T_j + 0.67283 \tag{6}$$

Table 1. $V_{ce\text{-}th}$ extraction at different junction temperatures.

Junction Temperature (°C)	a	b	R-Square	$V_{ce\text{-}th}$ (V)
30	5.46076	−3.48651	0.99852	0.6384
40	5.15092	−3.23811	0.99792	0.6286
50	5.3208	−3.28535	0.9975	0.6174
60	5.32871	−3.24046	0.99879	0.6081
70	5.34749	−3.20471	0.99878	0.5929

3.3. Acquisition of Package Voltage and On-State Chip Voltage

We tested the on-state voltage at different I_c and T_j values under an adequately heated condition using a high-low temperature test chamber. From the data we acquired from Figure 1, the intersection ($V_{ce\text{-}int}$) was marked, and the collector current at that point was denoted as $I_{c\text{-}int}$. When I_c was less than $I_{c\text{-}int}$, V_{ce} had a negative temperature coefficient because the $V_{ce\text{-}th}$ (negative temperature coefficient) represents the predominant part of the on-state voltage. When I_c was higher than $I_{c\text{-}int}$, the effect of the positive temperature coefficient ($V_{on\text{-}chip}$, $V_{package}$) increased and became the main position in the constituent part of the on-state voltage, and V_{ce} had a positive temperature coefficient.

The package resistance $R_{package}$ remained constant as I_c increased and had a positive temperature coefficient. Combined with the operating conditions of the experimental environment, Equation (4) was updated to Equation (7). In addition, $R_{package}$ was measured using the method described in reference [29]. This makes it possible to obtain $R_{package}$ at different junction temperatures; $V_{package}$ can be expressed by Equation (8). The curves of package voltage are shown in Figure 4:

$$R_{package}\left(T_j\right) = R_{package}\left(T_j = 25^\circ\mathrm{C}\right) \times \frac{228 + T_j}{228 + 25} \tag{7}$$

$$V_{package}\left(I_c, T_j\right) = R_{package}\left(T_j\right) \times I_c. \tag{8}$$

$V_{on\text{-}chip}$ was obtained after acquiring the information of V_{ce} and $V_{package}$, as shown in Figure 5. It had a positive temperature coefficient and increased as I_c increased. In this paper, we defined $F_{Von\text{-}chip}$ (I_c,T_j) to describe the on-state chip voltage at any collector current and junction temperature. The data we acquired were imported into MATLAB software and the fitting function was expressed as

$$F_{Von\text{-}chip}\,(I_c,T_j) = \mathrm{P}_{00} + \mathrm{P}_{10}I_c + \mathrm{P}_{01}T_j + \mathrm{P}_{20}{I_c}^2 + \mathrm{P}_{11}I_cT_j + \mathrm{P}_{30}{I_c}^3 + \mathrm{P}_{31}{I_c}^2T_j \tag{9}$$

where P_{00} is 0.1234, P_{10} is 0.00856, P_{01} is −0.0002294, P_{20} is -5.962×10^{-5}, P_{11} is 3×10^{-5}, P_{30} is 3.34×10^{-7}, P_{31} is 5.976×10^{-8}. The R-square value was 0.9988, indicating that the errors are within acceptable margins.

4. Prediction Result for Bond Wire Failure

4.1. Method of Applying On-State Voltage Separation Strategy to Predict Bond Wire Failure

Due to the differences in thermal expansion coefficients, IGBT module bond wires inevitably endure thermal stress under different working conditions. After a very large number of temperature cycles [30,31], the repeated stress–strain of the bond wires leads to the initiation and expansion of cracks at the solder joints, which eventually causes the bond wires to crack or liftoff. The destroyed bond wires accelerate the aging of other healthy bond wires and finally cause IGBT module failure.

Moreover, the aging of the bond wires increases the package resistance, $R_{package}$, and on-state voltage, V_{ce}. It is difficult to avoid fluctuations of I_c and T_j across the collector-emitter in the IGBT module, which should be eliminated when considering the bond wire aging effect on the on-state voltage.

Table 2 shows the influences of I_c, T_j, and aging on each part of the on-state voltage mentioned in Section 2. It can be seen from Table 2 that $V_{package}$ is the unique factor reflecting bond wire aging except for V_{ce} and serves as the origin of the increase in on-state voltage in the aging process of bond wires.

Table 2. Different factors in the components of on-state voltage.

Voltage	I_c (Increases)	T_j (Increases)	Bond Wire Failure
$V_{ce\text{-}th}$	—	↓	—
$V_{on\text{-}chip}$	↑	↑	—
$V_{package}$	↑	↑	↑

We then applied the separation strategy of on-state voltage to IGBT module bond wire failure prediction, as shown in Figure 9. $V_{ce\text{-}mea}$ is the on-state voltage measured under on-line conditions, and $V_{package\text{-}cal}$ is the package voltage calculated using Equation (10) under the same conditions after acquiring I_c and T_j information. $V_{package\text{-}hea}$, $V_{package\text{-}2liftoff}$, and $V_{pacakge\text{-}4liftoff}$ are the package voltages measured under off-line conditions (healthy, two bond wires liftoff, and four bond wires liftoff, respectively):

$$V_{package\text{-}cal} = V_{ce\text{-}mea} - V_{ce\text{-}th}\,(T_j) - V_{on\text{-}chip}\,(T_j, I_c). \tag{10}$$

According to the on-state voltage separation strategy proposed by us, V_{ce} was separated into $V_{ce\text{-}th}$ and $V_{on\text{-}chip}$, which remained constant throughout the IGBT module bond wire aging process, and $V_{package}$ which is the dependent variable in the process of bond wire aging. This separation strategy eliminates the interference of the independent variable and makes it possible to directly observe the voltage change caused by the bond wire failure.

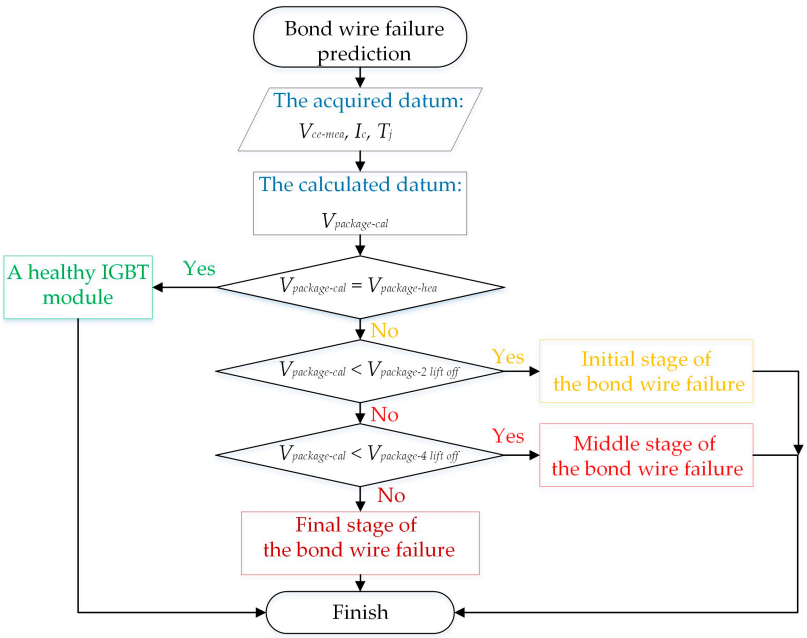

Figure 9. The method of applying on-state voltage separation strategy to bond wire failure prediction.

4.2. Accuracy of the Diagnosis Strategy in Predicting Bond Wire Failure

To study the parametric characteristics of the IGBT module after a bond wire failure, a reasonable method is necessary to accelerate the bond wire aging process. Power cycling [32] and bond wire cut off [33] are widely used in the aging of IGBT modules. The latter method simulates the different aging degrees by changing the sheared number of the bond wires and visually reflects the failure. What is more, the essence of IGBT module bond wire failure is the disconnection of two hitherto connected parts. Thus, applying the cut-off method to IGBT module bond wire failure simulation has no influence on the failure prediction scheme proposed in this paper. Therefore, this method was adopted to accelerate the aging process of bond wires.

In this paper, the on-state voltages for two bond wires cut off and four bond wires cut off were set as critical points between the different aging periods. The diagnostic strategy is shown in Figure 9 and examples are provided to verify the accuracy of the on-state voltage separation strategy in predicting the IGBT module bond wire failure.

$R_{package}$ has an obvious change in the bond wire aging process for the IGBT module. To acquire a precise standard for bond wire aging prediction, $R_{package}$ was tested using the equipment shown in Figure 6. The junction temperature was set to 25 °C, and $V_{ce\text{-}th}$ was obtained by Equation (6). The voltage supplied by a high-power source was increased gradually until the IGBT module reached the on-state status ($V_{ce} > V_{ce\text{-}th}$). The experimental data are presented in Table 3. Thus, $V_{package\text{-}2liftoff}$ and $V_{package\text{-}4liftoff}$ at different T_j (30–70 °C) were calculated as standards of bond wire failure prediction. The detailed data are shown in Figure 10 (I_c = 75A).

Table 3. $R_{package}$ at different aging periods (T_j= 25 °C).

Voltage (V)	V_{ce} (V)	I_c (A)	$V_{ce\text{-}th}$ (V)	$R_{package}$ (mΩ)
2 bond wires liftoff	0.6463	0.4877	0.6448	3.0757
4 bond wires liftoff	0.6478	0.5383	0.6448	5.5731

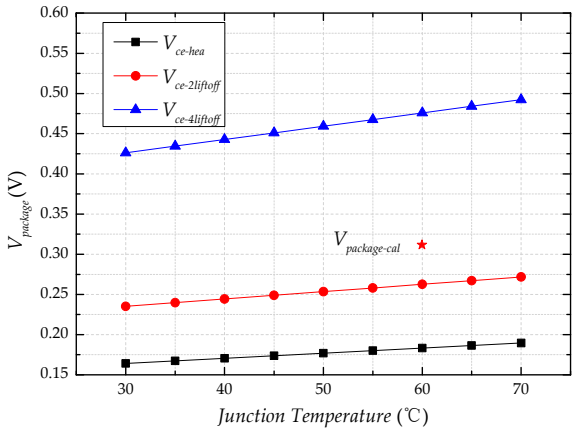

Figure 10. Package voltage at different junction temperature (I_c = 75 A).

To demonstrate the accuracy of our prediction method, different numbers of bond wires were cut off (1,3,5) and the results are shown for the following cases:

4.2.1. Case 1: One Bond Wire Cut Off, I_c = 75A, T_j = 50 °C

The IGBT module with one bond wire cut-off was tested, and the diagnosis process shown in Figure 11 was applied. The electronic load in Figure 6 was substituted with a high-power load (600 V/240 A/12 kW) to acquire a higher collector current (75 A). The diagnosis strategy shows that $V_{package\text{-}cal}$ is higher than $V_{package\text{-}hea}$, but lower than $V_{package\text{-}2liftoff}$. Thus, it can be classified as the initial stage of the bond wire failure, the same status as the real aging process.

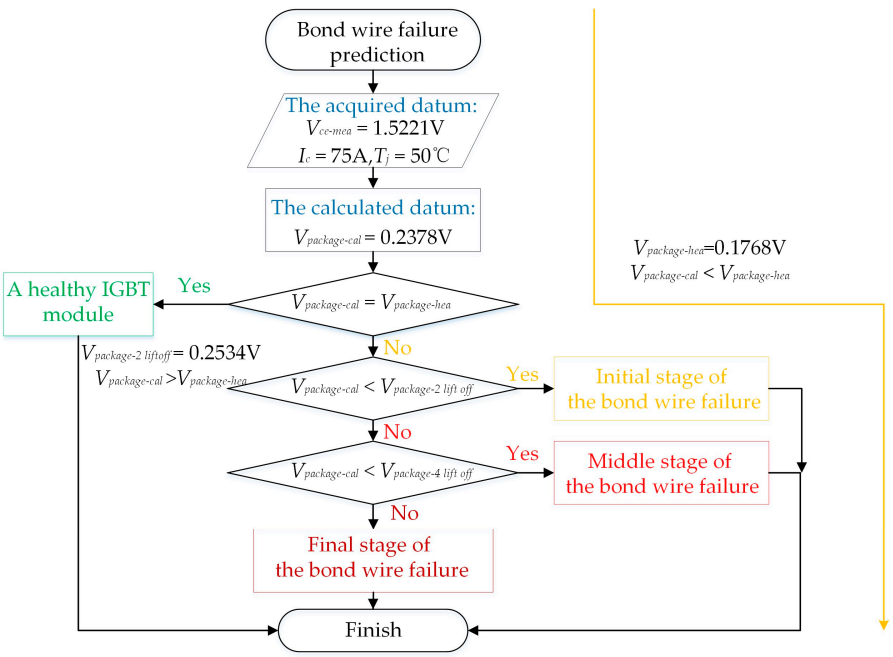

Figure 11. The diagnosis process for IGBT module bond wire failure.

4.2.2. Case 2: Three Bond Wires Cut Off, I_c = 75A, T_j = 60 °C

We then tested the on-state voltage of another IGBT module (three bond wires cut off). With I_c = 75 A and $V_{ce\text{-}mea}$ = 1.6091 V, Equations (6), (9) and (10) yield $V_{ce\text{-}th}$ = 0.6056 V, $V_{on\text{-}chip}$ = 0.6898 V, $V_{package\text{-}cal}$ = 0.3137 V, respectively, as shown in Figure 10. The diagnosis strategy shows it can be classified as the middle stage of the bond wire failure, the same status as the real aging process. Thus,

the aging process of bond wire can be predicted accurately at different junction temperatures using the proposed diagnosis strategy.

4.2.3. Case 3: Three Bond Wires Cut Off, I_c = 20 A, T_j = 60 °C

The research presented in this paper shows that $R_{package}$ is in the milli-ohm range, resulting in a low proportion of on-state voltage even under high current conditions. When it comes to low current conditions, $V_{package}$ will be lower than before. It is necessary to demonstrate the applicability of our diagnosis strategy under low current conditions.

When I_c is 20 A, $V_{ce\text{-}mea}$ is 0.9803 V, $V_{ce\text{-}th}$ is 0.6056 V, $V_{on\text{-}chip}$ is 0.2990 V, and $V_{package}$ is 0.0757 V which is marked in Figure 12. Thus, the middle stage of the bond wire failure can be diagnosed accurately by the proposed strategy even under low current conditions.

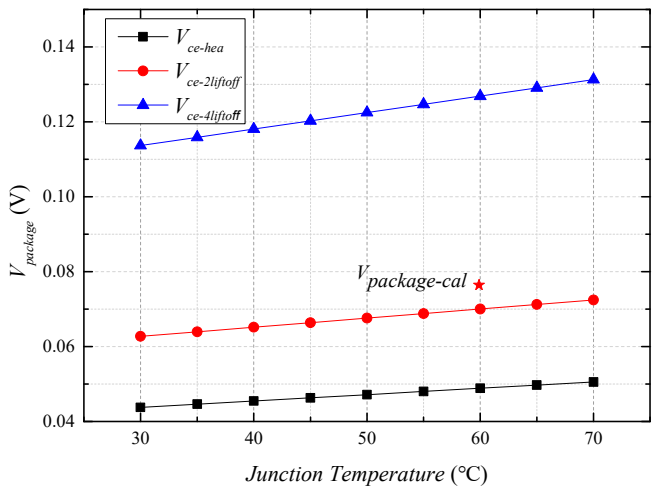

Figure 12. The package voltage at different junction temperatures (I_c = 20 A).

4.2.4. Case 4: Five Bond Wires Cut Off, I_c = 75 A, T_j = 70 °C

We finally tested an IGBT module with five bond wires cut off. It worked normally with a higher on-state voltage under the same condition as $V_{package\text{-}4liftoff}$ in the low current range. However, as the current increased, the heat generated in the bond wires caused the complete failure of the bond wire as shown in Figure 13: the remaining healthy bond wires lifted off rapidly under high current conditions, which is the final stage of bond wire failure.

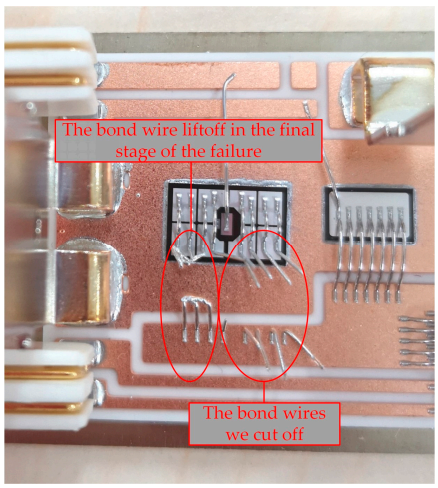

Figure 13. The final stage of bond wire failure.

5. Conclusions

In this paper, an IGBT module on-state voltage separation strategy based on physical structure has been proposed. This method considers the effect of collector current and junction temperature during the on-state status and gives a method to calculate for each part under different conditions.

This separation strategy eliminates the interference of the independent variable and makes it possible to directly observe the voltage changes caused by the bond wire failure. The experimental results demonstrate the effectiveness of the proposed diagnosis strategy in accurately predicting the bond wire failure stage in IGBT module under different conditions.

Author Contributions: Operation of the experiments, analysis and writing of the paper, Q.K.; guidance of theoretical analysis and writing, M.D.; guidance and optimizing of experiments, K.W.; modification of manuscript, Z.O. and W.G.H.

Funding: This research was funded by the "New Energy Vehicle" Key Special Project of the National Key Research and Development Plan [No. 2017YFB0102500]"and "the Tianjin Natural Science Foundation of China [No. 17JCYBJC21300]".

Conflicts of Interest: The authors declare no conflict of interest.

References

1. Li, H.; Hu, Y.; Liu, S.; Li, Y.; Liao, X.; Liu, Z. An Improved Thermal Network Model of the IGBT Module for Wind Power Converters Considering the Effects of Base Plate Solder Fatigue. *IEEE Trans. Device Mater. Reliab.* **2016**, *16*, 570–575. [CrossRef]
2. Alhmoud, L. Reliability Improvement for a High-Power IGBT in Wind Energy Applications. *IEEE Trans. Ind. Electron. Control Instrum.* **2018**, *65*, 7129–7137. [CrossRef]
3. Ji, B.; Pickert, V.; Cao, W.; Zahawi, B. In Situ Diagnostics and Prognostics of Wire Bonding Faults in IGBT Modules for Electric Vehicle Drives. *IEEE Trans. Power Electron.* **2013**, *28*, 5568–5577. [CrossRef]
4. Song, Y.; Wang, B. Evaluation Methodology and Control Strategies for Improving Reliability of HEV Power Electronic System. *IEEE Trans. Veh. Technol.* **2014**, *63*, 3661–3676. [CrossRef]
5. Zahedi, B.; Norum, L.E. Modeling and Simulation of All-Electric Ships With Low-Voltage DC Hybrid Power Systems. *IEEE Trans. Power Electron.* **2013**, *28*, 4525–4537. [CrossRef]
6. Cao, W.; Mecrow, B.C.; Atkinson, G.J.; Bennett, J.W.; Atkinson, D.J. Overview of Electric Motor Technologies Used for More Electric Aircraft (MEA). *IEEE Trans. Ind. Electrons.* **2012**, *59*, 3523–3531.
7. Yang, S.; Bryant, A.; Mawby, P.; Xiang, D.; Ran, L.; Tavner, P. An industry-based survey of reliability in power electronic converters. *IEEE Trans. Ind. Appl.* **2011**, *47*, 1441–1451. [CrossRef]
8. Blaabjerg, F.; Ma, K. Future on Power Electronics for Wind Turbine Systems. *IEEE J. Emerg. Select. Topic. Power. Elect.* **2013**, *1*, 139–152. [CrossRef]
9. Bie, X.; Qin, F.; An, T.; Zhao, J.; Fang, C. Numerical simulation of the wire bonding reliability of IGBT module under power cycling. In Proceedings of the International Conference on Electronic Packaging Technology, Harbin, China, 16–19 August 2017; pp. 1396–1401.
10. Fazeli, S.M.; Jovcic, D.; Hajian, M. Laboratory Demonstration of Closed-Loop 30KW, 200V/90V IGBT-Based LCL DC/DC Converter. *IEEE Trans. Power Delivery.* **2018**, *33*, 1247–1256. [CrossRef]
11. Luo, H.; Wang, X.; Zhu, C.; Li, W.; He, X. Investigation and Emulation of Junction Temperature for High-Power IGBT Modules Considering Grid Codes. *IEEE J. Emerg. Select. Topic. Power. Elect.* **2018**, *6*, 930–940. [CrossRef]
12. Bahman, A.S.; Ma, K.; Ghimire, P.; Iannuzzo, F.; Blaabjerg, F. A 3-D-Lumped Thermal Network Model for Long-Term Load Profiles Analysis in High-Power IGBT Modules. *IEEE J. Emerg. Select. Topic. Power. Elect.* **2016**, *4*, 1050–1063. [CrossRef]
13. Niu, H. The Effect of Load Properties on the Reliability of Machine Drives—The Temperature and Stress Analysis of Power Module Bond Wires. In Proceedings of the IEEE Energy Conversion Congress and Exposition, Cincinnati, OH, USA, 1–5 October 2017; pp. 2533–2539.
14. Choi, U.; Blaabjerg, F.; Jørgensen, S. Study on Effect of Junction Temperature Swing Duration on Lifetime of Transfer Molded Power IGBT Modules. *IEEE Trans. Power Electron.* **2017**, *32*, 6434–6443. [CrossRef]
15. Bahman, A.S.; Iannuzzo, F.; Uhrenfeldt, C.; Blaabjerg, F.; Stig, M. Modeling of Short-Circuit-Related Thermal Stress in Aged IGBT Modules. *IEEE Trans. Ind. Appl.* **2017**, *53*, 4788–4795. [CrossRef]

16. Smet, V.; Forest, F.; Huselstein, J.-J.; Rashed, A.; Richardeau, F. Evaluation of V_{ce} Monitoring as a Real-Time Method to Estimate Aging of Bond Wire-IGBT Modules Stressed by Power Cycling. *IEEE Trans. Ind. Electron.* **2013**, *60*, 2760–2770. [CrossRef]
17. Haque, M.S.; Choi, S.; Baek, J. Auxiliary Particle Filtering-Based Estimation of Remaining Useful Life of IGBT. *IEEE Trans. Ind. Electron.* **2018**, *65*, 2693–2703. [CrossRef]
18. Peng, Y.; Zhou, L.; Du, X.; Sun, P.; Wang, K.; Cai, J. Junction temperature estimation of IGBT module via a bond wires lift-off independent parameter VgE-np. *IET Power Electron.* **2018**, *11*, 320–328. [CrossRef]
19. Wang, Z.; Tian, B.; Qiao, W.; Qu, L. Real-Time Aging Monitoring for IGBT Modules Using Case Temperature. *IEEE Trans. Ind. Electron.* **2016**, *63*, 1168–1178. [CrossRef]
20. Sun, P.; Gong, C.; Du, X.; Peng, Y.; Wang, B.; Zhou, L. Condition Monitoring IGBT Module Bond Wires Fatigue Using Short-Circuit Current Identification. *IEEE Trans. Power Electron.* **2017**, *32*, 3777–3786. [CrossRef]
21. Haque, M.S.; Baek, J.; Herbert, J.; Choi, S. Prognosis of Wire Bond Lift-Off Fault of an IGBT Based on Multisensory Approach. In Proceedings of the IEEE Applied Power Electronics Conference and Exposition, Long Beach, CA, USA, 20–24 March 2016; pp. 3004–3011.
22. Han, J.; Ma, M.; Chu, K.; Zhang, X.; Lin, Z. In-Situ Diagnostics and Prognostics of Wire Bonding Faults in IGBT Modules of Three-Level Neutral-Point-Clamped Inverters. In Proceedings of the IEEE 8th International Power Electronics and Motion Control Conference, Hefei, China, 22–26 May 2016; pp. 3262–3267.
23. Pedersen, K.B.; Kristensen, P.K.; Pedersen, K.; Uhrenfeldt, C.; Munk-Nielsen, S. Vce as Early Indicator of IGBT Module Failure Mode. In Proceedings of the IEEE International Reliability Physics Symposium, Monterey, CA, USA, 2–6 April 2017; pp. FA-1.1–FA-1.6.
24. Ghimire, P.; Bęczkowski, S.; Munk-Nielsen, S.; Rannestad, B.; Thøgersen, P.B. A Review on Real Time Physical Measurement Techniques and Their Attempt to Predict Wear-Out Status of IGBT. In Proceedings of the European Conference on Power Electronics and Applications, Lille, France, 2–6 September 2013; pp. 1–10.
25. Hoeer, M.; Weiss, F.; Bernet, S. Online Collector-Emitter Saturation Voltage Measurement for the In-Situ Temperature Estimation of a High-Power 4.5 kV IGBT Module. In Proceedings of the European Conference on Power Electronics and Applicationsin, Warsaw, Poland, 11–14 September 2017; pp. 1–9.
26. Degrenne, N.; Mollov, S. On-line Health Monitoring of Wire-Bonded IGBT Power Modules Using On-State Voltage at Zero-Temperature-Coefficient. In Proceedings of the International Exhibition and Conference for Power Electronics, Intelligent Motion, Renewable Energy and Energy Management, Nuremberg, Germany, 5–7 June 2018; pp. 1–7.
27. Choi, U.; Blaabjerg, F. Separation of Wear-Out Failure Modes of IGBT Modules in Grid-Connected Inverter Systems. *IEEE Trans. Power Electron.* **2018**, *33*, 6217–6223. [CrossRef]
28. Halick, M.S.M.; Kandasamy, K.; Jet, T.K.; Sundarajan, P. Online Computation of IGBT On-State Resistance for Off-Shelf Three-Phase Two-Level Power Converter Systems. *Microelectron. Reliab.* **2016**, *64*, 379–386. [CrossRef]
29. Kong, Q.; Du, M.; Ouyang, Z.; Wei, K.; Hurley, W.G. A Model of the On-State Voltage across IGBT Modules Based on Physical Structure and Conduction Mechanisms. *Energies* **2019**, *12*, 851. [CrossRef]
30. Smet, V.; Forest, F.; Huselstein, J.J.; Richardeau, F.; Khatir, Z.; Lefebvre, S.; Berkani, M. Ageing and Failure Modes of IGBT Modules in High-Temperature Power Cycling. *IEEE Trans. Ind. Electron.* **2011**, *58*, 4931–4941. [CrossRef]
31. Tounsi, M.; Oukaour, A.; Tala-Ighil, B.; Gualous, H.; Boudart, B.; Aissani, D. Characterization of high-voltage IGBT module degradations under PWM power cycling test at high ambient temperature. *Microelectron. Reliab.* **2010**, *50*, 1810–1814. [CrossRef]
32. Ji, B.; Song, X.; Sciberras, E.; Cao, W.; Hu, Y.; Pickert, V. Multiobjective Design Optimization of IGBT Power Modules Considering Power Cycling and Thermal Cycling. *IEEE Trans. Power Electron.* **2015**, *30*, 2493–2504. [CrossRef]
33. Wei, K.; Du, M.; Xie, L.; Li, J. Study of Bonding Wire Failure Effects on External Measurable Signals of IGBT Module. *IEEE Trans. Device Mater. Reliab.* **2014**, *14*, 83–89.

© 2019 by the authors. Licensee MDPI, Basel, Switzerland. This article is an open access article distributed under the terms and conditions of the Creative Commons Attribution (CC BY) license (http://creativecommons.org/licenses/by/4.0/).